

A Malmquist-like bias in the inferred areas of diamond caustics and consequences for inferred time delays of gravitationally lensed quasars

DEREK M. BALDWIN¹ AND PAUL L. SCHECHTER^{1,2}

¹*MIT Department of Physics
Cambridge, MA 02139, USA*

²*MIT Kavli Institute for Astrophysics and Space Research
Cambridge, MA 02139, USA*

ABSTRACT

Quasars are quadruply lensed only when they lie within the diamond caustic of a lensing galaxy. This precondition produces a Malmquist-like selection effect in observed populations of quadruply lensed quasars, overestimating the true caustic area. The bias toward high values of the inferred logarithmic area, $\ln A_{inf}$, is proportional to the square of the error in that area, $\sigma_{\ln A}^2$. In effect, Malmquist’s correction compensates *post-hoc* for a failure to incorporate a prior into parameter optimization. Inferred time delays are proportional to the square root of the inferred caustic area of the lensing galaxy. Model time delays are biased long, leading to overestimates of the Hubble constant. Crude estimates of $\sigma_{\ln A}$ for a sample of 13 quadruple systems give a median value of 0.16.

We identify a second effect, “inferred magnification bias,” resulting from the combination of selection by apparent magnitude and errors in model magnification. It is strongly anti-correlated with caustic area bias, and almost always leads to underestimates of the Hubble constant. Malmquist’s scheme can be adapted to priors on multiple parameters, but for quad lenses, the negative covariances between caustic area and absolute magnitude are poorly known. Inferred magnification bias may even cancel out caustic area bias, depending upon (among other things) the slope of the number magnitude relation for the sample.

Proper correction for these combined effects can, in principle, be built into Bayesian modeling schemes as priors, eliminating the need for Malmquist-style approximation, but is likely to be challenging in practice.

Keywords: galaxies: quasars — gravitational lensing: strong, Malmquist bias, time delay cosmography

1. INTRODUCTION

The “era of precision cosmology” (e.g. [Kaplinghat & Turner 2001](#)) was widely heralded by cosmologists (but not all; see [Bridle et al. 2003](#)) and the occasional astronomer. Much of the precision in “precision cosmology” can be attributed to the high degree of homogeneity and small amplitude of perturbations in the early universe. But in today’s universe the populations of astronomical objects used for cosmological inference (e.g. Cepheid variable stars, type Ia supernovae, gravitation-

ally lensed quasars) exhibit wide ranges of properties that must be taken into full account. These properties introduce uncertainties that become all the more important with the ever-increasing precision of cosmological measurements.

In this paper we discuss systematic biases in the measurements of several quantities associated with gravitational lenses (specifically caustic area, time delay, and magnification) that depend on these uncertainties. We consider time delay measurements of quadruply lensed quasars, widely regarded as a high precision method for measurement of the Hubble constant, H_0 ([Refsdal 1964](#); [Treu & Marshall 2016](#); [Wong et al. 2020](#)). As is well-

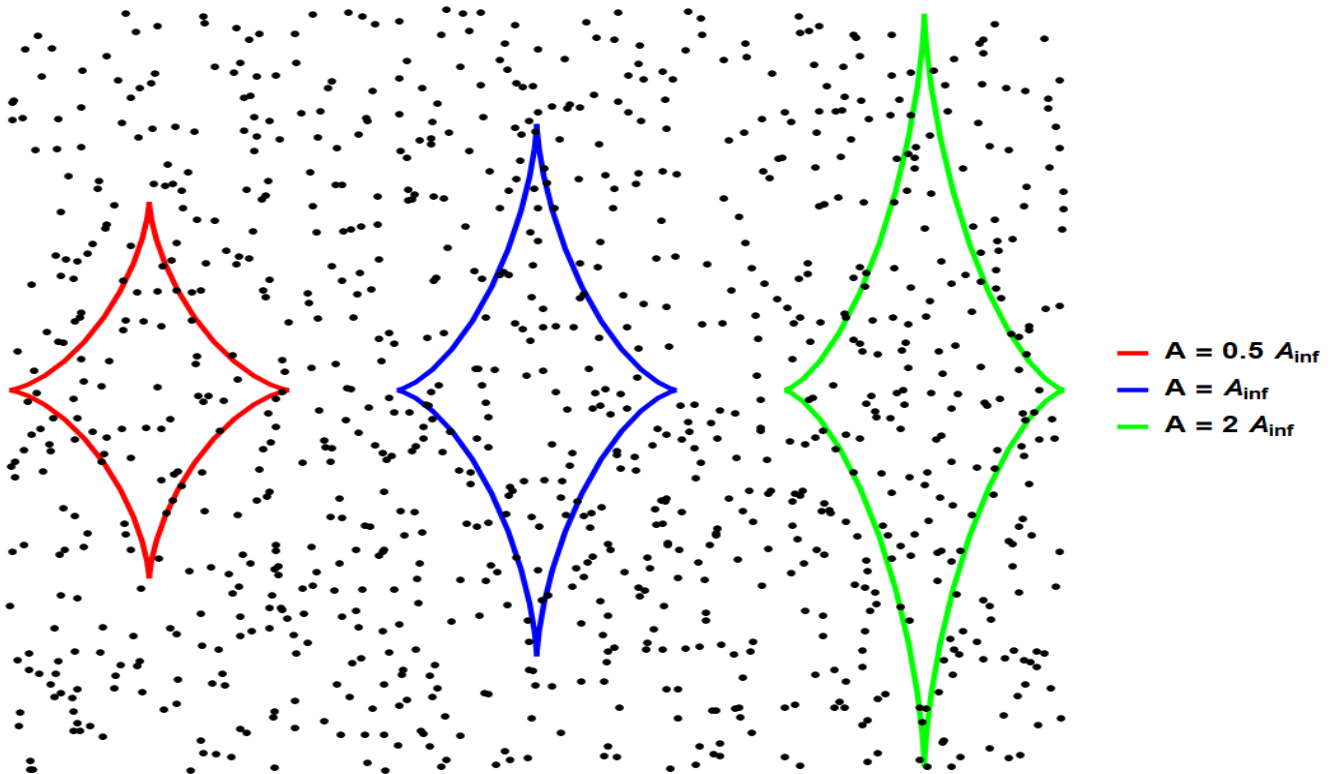


Figure 1. Plots of diamond caustics with areas $\ln A_{inf} \pm \sigma_{\ln A}$, where $\sigma_{\ln A} = \ln 2$, and randomly generated source quasar locations. Quads with higher caustic areas are over-represented in a sample because more source locations fall within the larger areas. The average caustic area for this sample of quads is $A_{peak} \approx 1.5 A_{inf}$.

known, these systems have a “diamond” or “astroidal¹” caustic (Ohanian 1983), which gives rise to a “quad” of images only when the source quasar is located inside this caustic (Finch et al. 2002). We demonstrate that this condition leads to an analogue of the well-known Malmquist effect (Malmquist 1922; Binney & Merrifield 1998), in which the true luminosities of stars in flux-limited samples are higher than inferred from their spectra due to a selection bias in the sample. In Section 2 we show how a similar selection effect occurs in the study of quadruply-lensed quasars, causing the true areas in “quadruplicity” selected samples to be lower than inferred from modeling observations of the lensed system. We call this “inferred caustic area bias.” In Section 6 we describe a thought experiment showing that there is no way to account for this bias without explicitly modeling it. In Section 7 we derive formulae for caustic areas for several idealized models. In Section 8 we use these to estimate inferred caustic area bias in two samples.

¹ Note that these caustics form perfect astroids only in special cases. The caustics considered here are almost, but not quite, stretched astroids.

While such an underestimate in the inferred caustic areas of lensing galaxies might seem benign, we argue in Section 6 that the area and associated relative time delay in the system are strongly correlated, so that such an underestimate of caustic area introduces an underestimate of the time delay for each system. We claim that this in turn creates a finite overestimate of the Hubble constant that must be accounted for when making precise measurements. In Section 7 we show how this affects the Hubble constant.

Finally, in Section 11, we summarize the results of Appendix B, showing how random uncertainties in the inferred magnification combine coherently with the uncertainties in inferred caustic area (for the restricted case of perfect anti-correlation) to alter the estimates obtained in the previous sections.

All of our estimates are made using Malmquist’s approximate, *post-hoc* approach to correcting the results of fitting schemes. Malmquist’s method grows increasingly unwieldy as one allows for pairs, triplets and higher order multiplets of mutually correlated parameters. Many of these shortcomings might be avoided, at least in principle, by incorporating the associated selection effects as Bayesian priors within model fitting schemes. But such

Bayesian schemes are often computationally expensive, and Malmquist’s approach permits a less expensive qualitative exploration of alternative schemes for computing caustic area bias.

2. THE MALMQUIST-LIKE EFFECTS FOR LENS CAUSTIC AREAS

2.1. *Classical Malmquist bias*

Malmquist’s original paper (Malmquist 1922) concerned the inferred and true intrinsic luminosities of stars included in a magnitude limited sample. The absolute magnitude of a star, M_{inf} , can be inferred from examination of its spectrum. But there is an error in that inferred magnitude, the amplitude of which is taken to vary randomly from one star to the next, distributed with a Gaussian of known width σ_M about some “true” absolute magnitude M .

While Malmquist allowed for non-uniformity, we assume for simplicity that the stars in the sample have constant spatial number density. We take the volume searched for a star with absolute magnitude M_{inf} to be V_{inf} . Then the volume searched for a brighter star with absolute magnitude $M_{inf} - \sigma_M$ will be larger by a factor of $\exp(2.3026\sigma_M)$ than V_{inf} , and stars with absolute magnitude $M_{inf} - \sigma_M$ will be over-represented in the sample by that same factor. Averaging over the distribution of uncertainties, one has

$$\langle M \rangle_{sample} = M_{inf} - 1.38\sigma_M^2, \quad (1)$$

The most important feature of this equation, distinguishing Malmquist’s effect from statistical errors, systematic instrumental errors, and systematic errors in the calibration of a distance indicator, is that it varies as the *square* of the error σ_M^2 . Secondly, it does not depend upon sample size. The Gaussian errors can make the true absolute magnitude brighter or fainter than M_{inf} . By contrast, Malmquist’s effect always makes the expected sample average brighter – even for a sample of one.

Binney & Merrifield (1998) give a thorough treatment of the effect. Our calculation of caustic area bias parallels their development in somewhat condensed form.

2.2. *Caustic area bias*

In the same way that uncertainties in the derived luminosities of stars cause the true luminosities of the stars in a magnitude-limited sample to be brighter than the derived luminosities, the uncertainty in the derived area of a lens caustic causes the true caustic area to be larger than the derived caustic area. This is due to the fact that a quasar cannot be quadruply-lensed unless the source lies within the diamond caustic (Finch

et al. 2002). The systems we see as “quads” are likely to have true astroidal caustic areas larger than inferred because lensing galaxies with true astroidal caustics that are 1 standard deviation larger than inferred are over-represented and lensing galaxies with true astroidal caustics that are 1 standard deviation smaller than inferred are under-represented. Since we select only systems with their source quasar located inside the diamond caustic, the probability that a system is included in a sample of “quads” is proportional to the true area of its caustic. This is illustrated in Figure 1.

The derivation here of the size of the effect is similar to the derivation of Malmquist’s effect in Binney & Merrifield (1998). We introduce a Gaussian distribution of systems with true caustic areas $\ln A$ about an inferred mean value $\ln A_{inf}$.

Then the contribution to the total number of observed quadruply-lensed systems, N , with respect to area is given by:

$$\frac{dN}{d \ln A} = \frac{n}{\sqrt{2\pi\sigma_{\ln A}^2}} \left(\frac{A}{A_{inf}} \right) \exp \left[\frac{-(\ln A - \ln A_{inf})^2}{2\sigma_{\ln A}^2} \right] \quad (2)$$

where n is a number density (numbers per steradian) and $\sigma_{\ln A}$ is the standard deviation in $\ln A$. The ratio A/A_{inf} gives the probability of observing a lens with true caustic area A relative to one with A_{inf} . Substituting $\exp(\ln A - \ln A_{inf})$ for A/A_{inf} and letting $\mathcal{N} = n/\sqrt{2\pi\sigma_{\ln A}^2}$ we have

$$\begin{aligned} \frac{dN}{d \ln A} &= \mathcal{N} \exp \left[\frac{-(\ln A - \ln A_{inf})^2}{2\sigma_{\ln A}^2} + (\ln A - \ln A_{inf}) \right] \\ &= \mathcal{N} \exp \frac{-(\ln A - \ln A_{inf} - \sigma_{\ln A}^2)^2 + \sigma_{\ln A}^4}{2\sigma_{\ln A}^2} \\ &= \mathcal{N} \exp \frac{\sigma_{\ln A}^2}{2} \exp \frac{-(\ln A - \ln A_{inf} - \sigma_{\ln A}^2)^2}{2\sigma_{\ln A}^2} \end{aligned}$$

which is a new Gaussian distribution with a shifted peak at

$$\ln A_{peak} = \ln A_{inf} + \sigma_{\ln A}^2. \quad (3)$$

We can then define the “logarithmic area bias”, $\Delta_{\ln A}$, that reflects this systematic error:

$$\Delta_{\ln A} \approx \ln A_{inf} - \ln A_{peak} = -\sigma_{\ln A}^2. \quad (4)$$

where A is the “true” caustic area that would be measured if there were no error in the imperfect caustic area inferred from the observations. The logarithmic mean of the caustic area inferred from observations is larger than the is larger than inferred by $\sigma_{\ln A}^2$ – the inferred caustic areas are underestimated. Similarly, Malmquist’s effect causes inferred intrinsic luminosities

to be underestimated – true absolute magnitudes are more negative

$$\Delta_M = M_{inf} - M_{peak} = 1.38\sigma_M^2, \quad (5)$$

where the factor of 1.38 is $\frac{3}{2} \ln 2.5$. In both cases, there is an additive bias in the logarithm of the relevant quantity – absolute magnitude in the Malmquist case and logarithmic caustic area for the quads – that is proportional to the square in the uncertainty in the logarithm of that quantity.

2.3. “Correction” or “Bias”

Malmquist (1922) cast his scheme as a “correction” to fluxes inferred from spectroscopy, and equation (5) gives that correction in magnitudes. Fifty years later, Rubin et al. (1976) brought Malmquist’s correction to bear on competing calculations of Hubble’s constant, which differed by a factor of two. They used the words “Malmquist bias” to describe the consequence of not including the correction.

While Malmquist’s “correction” scheme has fallen into disuse, the term Malmquist “bias” has considerable currency, quite often in discussions of the Hubble constant. Had we adhered to Malmquist’s terminology, we would have called the quantity defined in equation (5), Δ_M , the Malmquist *correction* and the quantity defined in equation (4), $\Delta_{\ln A}$, the logarithmic caustic area *correction*. Instead, in what follows, we refer to these quantities as *biases*, a decision we came to regret only after the paper had been refereed. Readers are asked to remember that though we call these quantities “biases”, they are actually “corrections,” and that a correction has a sign opposite that of a bias.

3. A BAYESIAN INTERPRETATION OF MALMQUIST’S CORRECTION

Malmquist’s correction may be interpreted as an attempt to account for what Bayesians would call a prior on the absolute magnitudes of stars selected by apparent magnitude. The prior has a simple mathematical form and, if one assumes a Gaussian distribution of absolute magnitudes, the effect on the mean absolute magnitude can be computed analytically.

Our calculation of caustic area bias is likewise a Bayesian correction for a sample prior, again under the assumption that the distribution of logarithmic caustic areas is Gaussian. Multiplying equation (2) by $\ln A$ we can likewise calculate the mean logarithmic caustic area by integrating.

While that integral can be done analytically, one could also do the integral using Monte Carlo methods, if one preferred. More generally, if the distribution of logarithmic caustic areas can be expressed analytically but

is not Gaussian, one might integrate using the trapezoidal rule or do Runge-Kutta integration. And again, it could also be done using Monte Carlo methods.

We have belabored what is obvious to most readers to emphasize that one need not use Monte Carlo methods to account for caustic area bias if one has a closed form solution for the caustic in terms of the model parameters.

4. MONTE CARLO CALCULATION OF CAUSTIC AREA BIAS

Figure 1 is, in effect, a Monte Carlo calculation of caustic area bias for three different caustic areas. We limited the range of source positions sampled to the boundaries of our plot.

Lens modelers often use Markov chain Monte Carlo (henceforth MCMC) methods (Sharma 2017) that preferentially sample parameter values in some neighborhood of the parameter values that are ultimately inferred. They must then account for that non-uniform sampling.

If the correction for non-uniform sampling is perfect, the MCMC modeling will have accounted for caustic area bias. But corrections for sampling bias are typically approximate, in which case there will be finite residual caustic area bias.

5. JOINT CALCULATION OF CAUSTIC AREA BIAS AND INFERRED MAGNIFICATION BIAS

Caustic area is strongly correlated with the magnifications inferred for quadruply lensed images, which depend upon multiple model parameters.

We discuss this at length in Section 11, but mention it here to indicate that Monte Carlo calculations must take that strong coupling into account in correcting for non-uniform sampling. The coupling of caustic area and inferred magnification will depend upon both source redshift and lens redshift. The priors for lens strength and intrinsic source luminosity are poorly known. Correction is challenging.

6. A GEDANKEN EXPERIMENT

We circulated a post-submission, pre-publication version of this paper and were surprised to find experts who thought that one or more of the elaborate lens modeling programs presently used by lens modelers might implicitly account for caustic area bias.

6.1. *Reductio ad absurdum*

We describe here a thought experiment that shows that if such an experiment *could* detect caustic area bias, it could also break the well known, mathematically exact

“mass sheet degeneracy” (Falco et al. 1985; Schneider & Sluse 2013). Stated simply, one cannot tell, from lensed images alone, whether or not a sheet of uniform mass surface density has been interposed between a source and an observer, on either the near or far side. This degeneracy can only be broken if one has additional information about either the source (perhaps a type Ia supernova) or the lens (e.g. by measuring the velocity dispersion of its stars).

We imagine a sample of gravitational lensed quasar systems each of which has the same six identical model parameters – an Einstein ring diameter, an isothermal radial mass profile with an ellipticity and a position angle, an external tidal shear with a different position angle, and a seventh, variable parameter, the true external convergence κ_{ext} . The source redshifts and lens redshifts are identical and each is known to infinite precision. We take the host galaxies to be identical and too small to be resolved. Source positions are distributed randomly.

The observations of the quasars are subject to measurement errors, which propagate to give uncertainties $\sigma_{\ln A}$ in the inferred logarithmic areas of the diamond caustics. As demonstrated in Section 2.2, the mean inferred logarithmic caustic area will be overestimated.

Our Gedanken systems differ only in the surface mass density, parameterized by the external convergence κ_{ext} , which is proportional to the surface mass density of a sheet in some fixed plane between the source and the observer. The logarithms of the convergences have a Gaussian distribution with dispersion $\sigma_{\ln \kappa_{ext}}^2$ about a mean value.

The area of the diamond caustic is proportional to $1/(1 - \kappa_{ext})^2$. If a lens modeling program could determine the area of the diamond caustic, it would break the mass sheet degeneracy.

6.2. Bayesian accounting for the mass sheet

Our Malmquist-like correction for the mass sheets assumes the Gaussianity of the distribution of logarithmic convergences. There is a straightforward (in principle) Bayesian alternative to Malmquist’s approach. If one adopts a prior proportional to the caustic area A in the modeling program, one can relax the assumption of Gaussianity and choose a different scheme for weighting different possible values for the convergence.

More generally, Malmquist’s method of correction may be thought of as using the derivative of the prior for some model parameter in the vicinity of its most likely value and the derived variance for that parameter to compute the effect of the prior.

7. CALCULATING CAUSTIC AREAS – IDEALIZED CASES

Though some lens modeling programs permit the plotting of the inferred diamond caustic, none of those known to the authors when this paper was first submitted produced areas for that caustic or uncertainties in that area.

This calculation is non-trivial. The tangential caustic is diamondlike if the lensing potential is symmetric about some axis, but is distorted if that symmetry is broken, say by the presence of external shear that is not aligned with the intrinsic flattening of the lens.

One can, however, derive approximate analytic expressions for several idealized cases. If the correctly calculated inferred caustic area is not too different from these, one might as a first guess use the scatter in these approximate caustic areas as a first guess for the uncertainty in the correctly calculated caustic area.

Alternatively, one can find the critical curve numerically, project it back onto the source plane and integrate either numerically or by Monte Carlo methods.

7.1. Singular isothermal potential in an external shear field

Finch et al. (2002) give an expression for the caustic area of a singular isothermal potential in an external shear field,

$$\psi(r, \theta) = br + \frac{\gamma r^2}{2} \cos 2\theta, \quad (6)$$

and find

$$A = \frac{3\pi}{2} b^2 \frac{\gamma^2}{1 - \gamma^2}. \quad (7)$$

This is one of the few lensing potentials for which an exact analytic solution is possible, and is a limiting case of the next potential we consider.

7.2. Singular isothermal elliptical potential with parallel external shear

Luhtaru et al. (2021) consider the SIEP + XS_{||} model,

$$\psi(r, \theta) = b \sqrt{q_{pot} x^2 + \frac{y^2}{q_{pot}}} - \frac{\gamma}{2} (x^2 - y^2). \quad (8)$$

They arrive at the approximate expression

$$A \approx \frac{3\pi b^2}{2} (\gamma + 2\eta)^2, \quad (9)$$

where η is the semi-ellipticity, $q_{pot} = (1 - \eta)/(1 + \eta)$. They rewrite this in terms of an “effective quadrupole,”

$$\Gamma_{eff} = \frac{\gamma + \eta}{1 + \gamma\eta}, \quad (10)$$

which is tightly constrained by the elongation of the image configuration. The parameter b , roughly the Einstein radius, θ_E , is also well constrained. But while Γ_{eff}

is well constrained, the ratio of the semi-ellipticity to the shear is usually much more poorly constrained.

Substituting for the semi-ellipticity, we get

$$A \approx \frac{3\pi\theta_E^2}{2} (2\Gamma_{eff} - \gamma)^2. \quad (11)$$

As the shear, γ , is more poorly constrained than the other parameters, it is the principal source of uncertainty in the caustic area. Taking the other parameters to be constant, an error in the shear, $\delta\gamma$, produces an error in the inferred logarithmic area, $\delta \ln A_{inf}$. We have

$$\delta \ln A_{inf} = \frac{2\delta\gamma}{(2\Gamma_{eff} - \gamma)}. \quad (12)$$

7.3. Power-law + external shear potential

Another manageable idealization is the power-law + external shear potential,

$$\psi(r, \theta) = br^\alpha + \frac{\gamma r^2}{2} \cos 2\theta, \quad (13)$$

which has Einstein radius $\theta_E = (b\alpha)^{1/(2-\alpha)}$. In Appendix A we calculate the approximate area of the diamond caustic for this case,

$$A \approx \frac{3\pi}{2} \theta_E^2 \gamma^2 \left(\frac{1}{1-\gamma^2} \right)^{\frac{1}{2-\alpha}}. \quad (14)$$

As noted previously, the Einstein radius is very well determined for any given system and so is relatively constant even as the slope is allowed to vary. However one expects strong covariance between the slope and external shear.

8. PRACTICAL UNCERTAINTIES IN CALCULATED CAUSTIC AREAS

We use two alternative schemes for modeling the typical uncertainty in the logarithmic area from equation (12). The first of these was developed by Luhtaru et al. (2021), who modeled the image and galaxy positions of 39 quasars lensed by relatively isolated galaxies with an isothermal elliptical potential with external shear parallel to the ellipticity (henceforth SIEP + XS_{||}). They report shear, semi-ellipticity, effective shear Γ_{eff} and approximate errors in the shear. Using equation (12) we calculate uncertainties in logarithmic caustic area, $\delta \ln A_{inf}$ and find a median value of 0.321.

Alternatively, we use the results of Shajib et al. (2019), who automated their modeling to give hands-off models for 13 quadruply lensed quasars, reporting model parameters and uncertainties for shears and mass axis-ratios, each with a distinct orientation. As equation (12) was derived for the case of shear parallel to ellipticity, we

add the shear and semi-ellipticity as spinors (Luhtaru et al. 2021) and consider only their projected components. Covariances were not reported, so we take the uncertainties in the shear and semi-ellipticity to be uncorrelated. Incorporating these into equation (12), we get a median uncertainty in the logarithmic caustic area of $\delta \ln A_{inf} = 0.16$.

As might be expected, the uncertainties from this alternative model (henceforth referred to as Bayesian) are somewhat smaller than for the SIEP + XS_{||} model. The Bayesian model has more free parameters than the latter, allowing for better fits to the image position data. We note, however, that equation (12) was derived under the assumption that projected shear and projected semi-ellipticity are perfectly anti-correlated. Proper accounting of actual covariances would have different effects on different systems.

A second reason to expect the Bayesian model to yield smaller uncertainties is that it uses the extended structure of the quasar hosts to constrain the model.

The approximations we used to estimate the uncertainties in inferred caustic areas were crude. To do better, one would need to find the critical curve, project it back onto the source plane and integrate numerically in the course of carrying out the Bayesian calculation, so as to account for of the covariance of shear and central concentration discussed in Section 7.3.

Summarizing our alternative schemes, we get uncertainties in the inferred logarithmic caustic area of

$$\delta \ln A_{inf} = \begin{cases} 0.32 \text{ (SIEP + XS}_{||}\text{)} & \text{or} \\ 0.16 \text{ (Bayesian)} & \end{cases}. \quad (15)$$

9. IMPLICATIONS OF CAUSTIC AREA BIAS FOR TIME DELAYS AND THE HUBBLE CONSTANT

9.1. Varying power-law slope

We examine 3 different systems that figure prominently in recent TDCOSMO results (Birrer et al. 2020): HE0435–1223, WFI2033–4723, and PG1115+080, and examine how the variation in the area of the diamond caustic influences time delay. We adopt the power-law + external shear lensing potential of equation (13), as implemented in Keeton’s `lensmodel` program (Keeton 2001).

While `lensmodel` permits the specification of a fiducial Hubble constant and redshifts for the lens and source, we use the program in its dimensionless mode.

1. For each of the 3 systems, we find the lens model that best fits the observations (image/galaxy position, image fluxes, etc.), all with a power-law slope (α) value of 1.

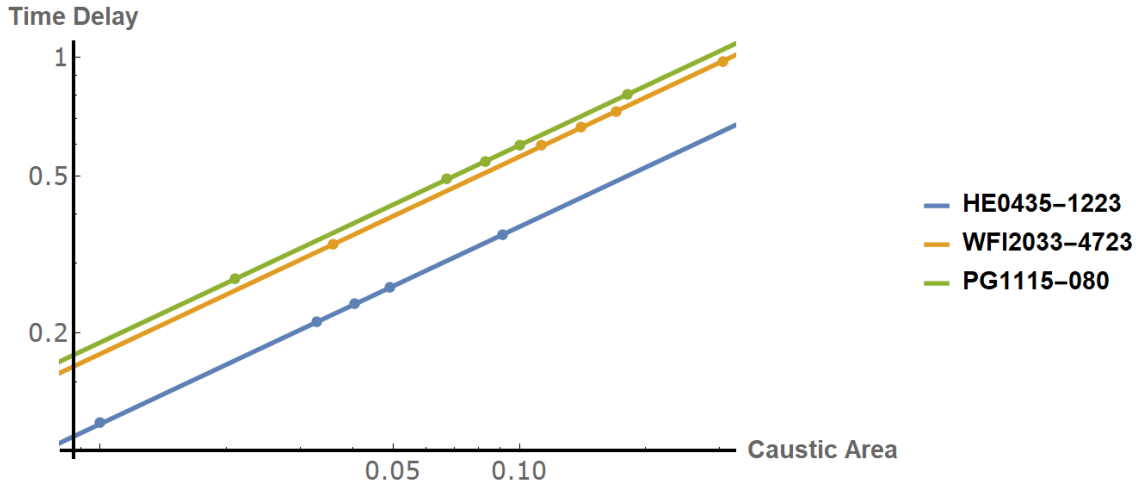


Figure 2. Log-Log Plots for Caustic Area (A) vs. Time Delay (τ) with lines of best fit. Each line of best fit has slope $\frac{1}{2}$.

2. We then create fictitious “perfect twin systems” with image positions, fluxes, etc. altered to exactly match the simulated values from `lensmodel`. This removes uncertainties due to image/galaxy positions so as to isolate the effect of changes in α on caustic area.
3. We next construct new models for each system with set α values of 0.5, 0.9, 1.0, 1.1, and 1.5. Each new model is generated with the “perfect twin” data values for the positions, fluxes, etc. This creates different-sized diamond caustics with areas given by equation (14).
4. Finally we find the time delays for each of these modeled systems. The caustic areas are calculated numerically from the curves generated by `lensmodel`.

The results for each of the 3 systems are contained below in Table 1 and Figure 2.

Table 1. Areas and Time Delays for HE0435-1223, WFI2033-4723, and PG1115+080

| α | HE0435-1223 | | WFI2033-4723 | | PG1115+080 | |
|----------|-------------|--------|--------------|--------|------------|--------|
| | A | τ | A | τ | A | τ |
| | $(\mu)^2$ | (Time) | $(\mu)^2$ | (Time) | $(\mu)^2$ | (Time) |
| 0.5 | 0.0913 | 0.3544 | 0.305 | 0.9740 | 0.181 | 0.8048 |
| 0.9 | 0.0491 | 0.2605 | 0.170 | 0.7278 | 0.100 | 0.5975 |
| 1.0 | 0.0405 | 0.2370 | 0.140 | 0.6640 | 0.083 | 0.5444 |
| 1.1 | 0.0328 | 0.2134 | 0.113 | 0.5994 | 0.067 | 0.4909 |
| 1.5 | 0.0100 | 0.1187 | 0.036 | 0.3354 | 0.021 | 0.2739 |

We see in Figure 2 that all three cases have a straight line log-log plot with slope 0.5 ± 0.01 . Without further proof, we shall assume that the time delay follows the relationship $\tau \propto \sqrt{A}$. If, as we have argued, the inferred caustic area is overestimated, the inferred time delay is also overestimated.

9.2. The effects of external convergences on time delays

The diamond caustic is larger when there is a positive external convergence than it would otherwise be. But the value of such a convergence is completely indeterminate, a consequence of the mass sheet degeneracy (Falco et al. 1985; Schneider & Sluse 2013), unless non-lensing observations (i.e. counts of nearby galaxies or measurements of the stellar velocity dispersion in the lens) are brought into the modeling. The position of the source *relative* to the diamond caustic remains unchanged by an external convergence. (Falor & Schechter 2022). The path lengths inferred from the lensing observations are therefore all too short by a factor $(1 - \kappa_{ext})$, and the inferred time delays are likewise too long by the same factor.

As inferred lengths scale as $(1 - \kappa_{ext})$, the inferred area of the diamond caustic is too small by the factor $(1 - \kappa_{ext})^2$. The inferred time delay scales as the square root of the inferred area, as was found experimentally for the case of the power-law potential with external shear in Section 9.1.

10. THE EFFECT OF CAUSTIC AREA BIAS ON THE HUBBLE CONSTANT

As discussed in Section 8, the results of Luhtaru et al. (2021) give uncertainties in the logarithmic caustic area $\delta \ln A_{inf} \approx 0.32$, while the results of Shajib et al. (2019)

give uncertainties $\delta \ln A_{inf} \approx 0.16$. From equation (4) we have

$$\Delta \ln A \approx \frac{\ln A_{inf}}{\ln A} \approx \begin{cases} -0.10 \text{ (SIEP + XS}_{\parallel}\text{)} & \text{or} \\ -0.025 \text{ (Bayesian)} & \end{cases} . \quad (16)$$

Note that $\Delta \ln A$, as defined in equation (4) and discussed in Section 2.3, is the *correction* to the inferred logarithmic caustic area that Malmquist would have computed. It is negative.

We argued in Section 9.1 that if the inferred caustic area is overestimated, the time delay inferred from a perfectly measured time delay, τ_{obs} is also overestimated, with

$$\frac{\ln \tau_{inf}}{\ln \tau_{obs}} = \frac{1}{2} \frac{\ln A_{inf}}{\ln A} . \quad (17)$$

This leads to a positive bias in the inferred value of the Hubble constant. We have

$$\frac{\ln H_0^{inf}}{\ln H_0^{true}} \approx -\frac{1}{2} \frac{\ln A_{inf}}{\ln A_{true}} \approx \begin{cases} 0.05 \text{ (SIEP + XS}_{\parallel}\text{)} & \text{or} \\ 0.012 \text{ (Bayesian)} & \end{cases} . \quad (18)$$

Hence the bias in the logarithm of the Hubble constant has the same amplitude but the opposite sign as the bias in the time delay. This is small compared to the random uncertainties in the reported measurements of H_0 , but it is systematic, and its sign is always positive. At such time as modelers estimate the caustic area in the course of their modeling, we will have a better estimate of its effect. And as noted in Section 6, one can then put a prior on caustic area that obviates the need for Malmquist’s correction.

In Section 8 we estimated the typical uncertainty in the logarithmic caustic area for the models of Luhtaru et al. (2021) and Shajib et al. (2019), respectively. Equation (12), used in producing these estimates, falls short for all of the systems in both papers, in some cases badly. One cannot properly calculate the uncertainty in the caustic area without properly calculating the caustic area itself within the modeling program. The difference between the SIEP + XS_∥ estimate and the Bayesian estimate gives some sense of the residual systematic error in the derived Hubble constant.

11. THE DEPENDENCE OF INFERRED CAUSTIC AREA BIAS ON THE ANTI-CORRELATION OF AREA AND MAGNIFICATION

In the preceding sections, we argued that when modeling a sample of quadruply lensed quasar systems, the average true area of their diamond caustics will be systematically larger than their average inferred area, by an amount approximately proportional to the *square*

of the typical individual error. This systematic error is the result of individual systems with positive errors ($\ln A - \ln A_{inf}$) being quadruply lensed more often than those with negative errors.

There is a *class* of systematic errors of this nature, the archetype of which was identified by Malmquist (1922), who considered the inferred absolute magnitudes for stars in a magnitude limited sample.

We consider here another such systematic error associated with the inferred magnifications of models for lensed quasars. It is the result of systems with positive magnification errors ($\mu - \mu_{inf}$) penetrating further into the rising number-magnitude relation for quasars than those those with negative errors.

The immediate temptation is to use Malmquist’s method to make a crude estimate of an “inferred magnification bias”.² But magnification and caustic area are in general strongly anti-correlated. They are, for example, inversely proportional to each other as one varies the convergence of a mass sheet. Proper treatment requires knowledge of the covariance of caustic area and magnification, and most likely other model parameters as well.

Malmquist’s approach is poorly suited to this “correlated area-magnification bias”. It might be more effectively addressed by the inclusion of a Bayesian prior in the modeling program, as suggested in Section 6.2.

Notwithstanding its shortcomings, Malmquist’s method yields an important conclusion: that the bias due to selection by apparent magnitude tends to mitigate the effects of selection by caustic area.

In Appendix B we derive expressions for the systematic errors in the inferred magnification and the inferred caustic area, under the following assumptions:

- Caustic area and magnification are perfectly anti-correlated, with $A \propto \mu^{-1/\alpha}$ and $\alpha > 0$,
- the redshifts of the lens and source are known,
- the number magnitude relation in the vicinity of m_{inf} , the apparent magnitude associated the inferred magnification μ_{inf} is given by $dN/dm \propto 10^{\beta(m-m_{inf})}$ (which increases at fainter apparent magnitudes for $\beta > 0$) and
- the errors in μ_{inf} are Gaussian.

For the caustic area, we find

$$\ln A_{peak} = \ln A_{inf} - \sigma_{\ln A}^2 + 2.5\beta\alpha\sigma_{\ln A}^2 , \quad (19)$$

² This is not to be confused with “magnification bias”, the term introduced by Turner (1980) to explain why the ratio of lensed quasars to unlensed quasars is higher at brighter apparent magnitudes.

which agrees with equation (3) if $\beta = 0$, corresponding to a flat number-magnitude relation.

For a rising number-magnitude relation, $\beta > 0$, ignoring the use of apparent magnitude to select a sample of quads causes the inferred caustic area bias (as computed in the previous sections) to be *overestimated*.

For the purpose of illustration (but not imitation) suppose $\beta = 0.3$ as might be appropriate for recently discovered quadruply lensed quasars. Suppose further that $\alpha = 1$, as would be appropriate if the errors in inferred magnification were due to uncertainty in the intervening mass sheet. The bias in the inferred logarithmic caustic area is then smaller by a factor of four than it would have been had magnification not been taken into account.

The slope β characterizing the number-magnitude relation is unlikely to be the same for different classes of lensed sources. For example, magnitude selected samples of quasars and supernovae are likely to have different systematic errors.

12. CONCLUSION

We have shown that, on average, the galaxies lensing quads will have inferred caustic areas biased low with respect to the true caustic areas. This results from the proportionality of cross section for quadruplicity to caustic area. We presented a *Gedanken* experiment to establish that the effect is inescapable. We have used Malmquist’s approximate method to estimate the amplitude of the effect for two sets of published model results.

There is a straightforward relationship between the caustic area of a given system and its associated time

delay, $\tau \propto \sqrt{A}$. A systematic bias in the inferred caustic areas produces a systematic bias in the inferred time delay. As the Hubble constant is inversely proportional to the inferred time delay, this bias low in area introduces a systematic underestimate of the inferred Hubble constant.

This inferred caustic area bias is mitigated by a second Malmquist-like bias due to errors in inferred model magnifications and the selection of systems by apparent magnitude. It appears to act oppositely to the caustic area bias, combining to produce a smaller net effect because caustic area and magnification are anti-correlated. Malmquist’s approximate *post-hoc* correction scheme is ill-suited to deal with correlated parameters. One can, for sufficiently restrictive cases, calculate approximate corrections for the two selection effects from reported uncertainties in (and reported covariances for) the model parameters, but these are of limited practical use.

As an alternative to Malmquist’s approach, one might in principle incorporate Bayesian priors for caustic area and magnification directly into model fitting programs, if the added computation does not prove to be prohibitive.

ACKNOWLEDGEMENTS

The authors thank an anonymous referee for noting that Bayesian Monte Carlo methods have the effect of correcting, albeit incompletely, for caustic area bias. The authors thank Richard Luhtarv and Drs. Philip Marshall, Sherry Suyu and Thomas Collett for comments on the manuscript. DB thanks the MIT UROP program for its support.

APPENDIX

A. APPROXIMATE CAUSTIC AREA FOR A POWER LAW + EXTERNAL SHEAR POTENTIAL

Here we follow closely the development in Finch et al. (2002) to derive an approximate analytic expression for astroidal caustic areas. We begin with the lensing potential:

$$\psi(r, \theta) = br^\alpha + \frac{\gamma r^2}{2} \cos 2\theta. \quad (\text{A1})$$

In Cartesian form:

$$\begin{aligned} \psi(x, y) &= b(x^2 + y^2)^{\frac{\alpha}{2}} + \frac{\gamma(x^2 + y^2)}{2} \cos 2 \arctan \frac{y}{x} \\ &= b(x^2 + y^2)^{\frac{\alpha}{2}} + \frac{\gamma}{2}(x^2 - y^2). \end{aligned} \quad (\text{A2})$$

The astroidal caustic is the locus of points for which the determinant of the inverse magnification matrix,

$$\mu^{-1} = \left(1 - \frac{\partial^2 \psi}{\partial x^2}\right) \left(1 - \frac{\partial^2 \psi}{\partial y^2}\right) - \left(\frac{\partial^2 \psi}{\partial x \partial y}\right) \quad (\text{A3})$$

disappears.

As for the shape of the caustic, according to An & Evans (2006), the “series [for the area] are also Taylor-series

expansions with respect to γ at $\gamma = 0$. If we truncate the expansion of the caustic after [the first] term, the expression reduces to the equation of the tetra-cuspi-hypocycloid, or the astroid.” We make the simplifying assumption that $\gamma \ll 1$, so as to simplify the expression to that of approximately an astroid. The area of an astroid is given by

$$A = \frac{3\pi}{8} x_c y_c, \quad (\text{A4})$$

where x_c and y_c are the x and y intercepts of the caustic (Finch et al. 2002). In what follows we consider only the intercepts of the caustic. Ignoring the cross term, which goes to zero on the axes, we are left with:

$$\begin{aligned} \mu^{-1} = & \left\{ 1 - b [x_c^2 + y_c^2]^{\frac{\alpha-4}{2}} [\alpha y_c^2 + \alpha(\alpha-1)x_c^2] - \gamma \right\} \\ & \times \left\{ 1 - b [x_c^2 + y_c^2]^{\frac{\alpha-4}{2}} [\alpha x_c^2 + \alpha(\alpha-1)y_c^2] + \gamma \right\} \end{aligned} \quad (\text{A5})$$

For a source at a cusp, the magnification at the corresponding point in the image plane is infinite in the direction transverse to that point’s displacement from the center of the lens. For a cusp on the x -axis, the magnification is infinite in the y -direction. Hence the $1 - \partial^2\psi/\partial y^2$ factors in equations (A3) and (A5) must be zero, giving

$$0 = 1 - b\alpha x_c^{\alpha-2} + \gamma, \quad (\text{A6})$$

and

$$x_c = \pm b^{\frac{1}{2-\alpha}} \left(\frac{\alpha}{1+\gamma} \right)^{\frac{1}{2-\alpha}}. \quad (\text{A7})$$

A parallel calculation for the y -intercept gives us

$$y_c = \pm b^{\frac{1}{2-\alpha}} \left(\frac{\alpha}{1-\gamma} \right)^{\frac{1}{2-\alpha}}. \quad (\text{A8})$$

Remapping back to the source plane via the lens equation,

$$\vec{r} - \vec{r}_s = \nabla\psi(\vec{r}), \quad (\text{A9})$$

we get

$$x_a = x_c (1 - b\alpha x_c^{\alpha-2} - \gamma) \quad (\text{A10})$$

$$= -2\gamma x_c \quad (\text{A11})$$

$$= \pm 2\gamma b^{\frac{1}{2-\alpha}} \left(\frac{\alpha}{1+\gamma} \right)^{\frac{1}{2-\alpha}}. \quad (\text{A12})$$

The same process for the y -intercept yields

$$y_c = \pm 2\gamma b^{\frac{1}{2-\alpha}} \left(\frac{\alpha}{1-\gamma} \right)^{\frac{1}{2-\alpha}}. \quad (\text{A13})$$

By the assumption $\gamma \ll 1$, we know the area of the caustic is proportional to the product of these two intercepts. The constant of proportionality for an astroid shape is $3\pi/8$. Thus we arrive at the final expression

$$A = \frac{3\pi}{2} \gamma^2 b^{\frac{2}{2-\alpha}} \left(\frac{\alpha^2}{1-\gamma^2} \right)^{\frac{1}{2-\alpha}}. \quad (\text{A14})$$

B. SYSTEMATIC EFFECTS DUE TO ERRORS IN INFERRED MAGNIFICATION

As outlined in Section 11, the application of Malmquist’s method to approximate the bias in inferred magnification and the resulting inferred time delay is more complicated than for inferred caustic area bias.

We make the following assumptions:

- Caustic area and magnification are perfectly anti-correlated with $A \propto \mu^{-1/\alpha}$, $\alpha > 0$,
- The redshifts of the lens and source are known,
- The number magnitude relation in the vicinity of m_{inf} , the apparent magnitude associated the inferred magnification μ_{inf} , is given by $dN/dm \propto 10^{\beta(m - m_{inf})}$ with the expectation that $\beta > 0$ and
- The errors in μ_{inf} are Gaussian.

We briefly suppress the additional complication of caustic area bias. We assume that the sample is comprised of lensed quasars with the same observed apparent magnitude m_{obs} over some small range $\pm \mathcal{D}m_{obs}$ and that we have selected a subsample of these that all have the same inferred logarithmic magnification $\ln \mu_{inf}$ over some small range $\pm \mathcal{D} \ln \mu_{inf}$. This is the analogue, in Malmquist’s treatment, of choosing all the stars with the same absolute magnitude, as inferred from spectroscopy. The unmagnified inferred apparent magnitude of the lens sample members is then

$$m_{inf} = m_{obs} + 2.5 \log \mu_{inf} = m_{obs} + 1.0857 \ln \mu_{inf} \quad . \quad (\text{B15})$$

Two factors influence the ratio of the probability $P(\ln \mu)$ of true logarithmic magnification $\ln \mu$ to the probability $P(\ln \mu_{inf})$ of inferred logarithmic magnification $\ln \mu_{inf}$.

The first of these reflects errors in determining $\ln \mu_{inf}$ from the available data, which we take to be a Gaussian with variance $\sigma_{\ln \mu}$.

The second of these arises from the number-magnitude relation,³ which we take to be a power law in received flux, of the form $10^{\beta(m - m_{inf})}$.

Taken together, we have the probability of logarithmic magnification $P(\ln \mu)$ in terms of the probability of the inferred logarithmic magnification $P(\ln \mu_{inf})$,

$$\frac{P(\ln \mu)}{P(\ln \mu_{inf})} = \left[10^{1.0857\beta(\ln \mu - \ln \mu_{inf})} \right] \exp \left[\frac{-(\ln \mu - \ln \mu_{inf})^2}{2\sigma_{\ln \mu}^2} \right]. \quad (\text{B16})$$

The number-magnitude term has the effect of favoring larger values of μ/μ_{inf} , in the same way the A/A_{inf} term in Section 2.2, favors larger caustic areas. If magnification and caustic area were uncorrelated, one might use this to compute an “inferred magnification bias” – distinct from the the “magnification bias” identified by Turner (1980) which results from decreasing β with fainter apparent magnitudes.

Instead we incorporate a factor for the caustic area bias that we have heretofore suppressed and proceed to compute a “correlated area-magnification bias.”

$$\frac{P(\ln \mu)}{P(\ln \mu_{inf})} = \left[\frac{A}{A_{inf}} \right] \left[10^{1.0857\beta(\ln \mu - \ln \mu_{inf})} \right] \exp \left[\frac{-(\ln \mu - \ln \mu_{inf})^2}{2\sigma_{\ln \mu}^2} \right]. \quad (\text{B17})$$

Adopting our assumption of perfect inverse correlation between magnification and caustic area, we have

$$\frac{P(\ln \mu)}{P(\ln \mu_{inf})} = \left[\frac{\mu}{\mu_{inf}} \right]^{-1/\alpha} \left[10^{1.0857\beta(\ln \mu - \ln \mu_{inf})} \right] \exp \left[\frac{-(\ln \mu - \ln \mu_{inf})^2}{2\sigma_{\ln \mu}^2} \right]. \quad (\text{B18})$$

Incorporating all of these into a single exponential, we have

$$\frac{P(\ln \mu)}{P(\ln \mu_{inf})} = \exp \left\{ \frac{1}{2\sigma_{\ln \mu}^2} \left[-\frac{2}{\alpha} \sigma_{\ln \mu}^2 (\ln \mu - \ln \mu_{inf}) + 5\beta \sigma_{\ln \mu}^2 (\ln \mu - \ln \mu_{inf}) - (\ln \mu - \ln \mu_{inf})^2 \right] \right\}. \quad (\text{B19})$$

³ As we have assumed that the redshift of the source is known, the number-magnitude relation is entirely determined by the luminosity function, sidestepping the additional complications of angular diameter distances.

As in Section 2.2 we can complete the square in the square brackets, giving a Gaussian whose peak value is shifted by the two power law terms.

$$\ln \mu_{peak} = \ln \mu_{inf} - \frac{1}{\alpha} \sigma_{\ln \mu}^2 + 2.5\beta \sigma_{\ln \mu}^2 \quad . \quad (\text{B20})$$

In the (unrealistic) limiting case where the caustic area becomes independent of the magnification, $\frac{1}{\alpha} \rightarrow 0$, equation (B20) reduces to the usual Malmquist correction, but with uncertainties in $\ln \mu$ instead of in magnitudes.

Alternatively, starting with Gaussian errors in caustic area, we have

$$\ln A_{peak} = \ln A_{inf} - \sigma_{\ln A}^2 + 2.5\beta\alpha \sigma_{\ln A}^2 \quad , \quad (\text{B21})$$

which would agree with equation (3) in the limit of $\beta = 0$, a flat number-magnitude relation.

Equations (B20) and (B21) give a sense of how inferred caustic area bias and inferred magnification bias compensate for each other for the case of perfect anti-correlation. As the parameter α depends upon the adopted lens model and the parameter β depends on details of the sample selection, the extent of that compensation must be determined on a case by case basis.

REFERENCES

- An, J. H., & Evans, N. W. 2006, *MNRAS*, 369, 317, doi: [10.1111/j.1365-2966.2006.10303.x](https://doi.org/10.1111/j.1365-2966.2006.10303.x)
- Binney, J., & Merrifield, M. 1998, *Galactic Astronomy* (Princeton University Press)
- Birrer, S., Shajib, A. J., Galan, A., et al. 2020, *A&A*, 643, A165, doi: [10.1051/0004-6361/202038861](https://doi.org/10.1051/0004-6361/202038861)
- Bridle, S. L., Lahav, O., Ostriker, J. P., & Steinhardt, P. J. 2003, *Science*, 299, 1532, doi: [10.1126/science.1082158](https://doi.org/10.1126/science.1082158)
- Falco, E. E., Gorenstein, M. V., & Shapiro, I. I. 1985, *ApJL*, 289, L1, doi: [10.1086/184422](https://doi.org/10.1086/184422)
- Falor, C., & Schechter, P. L. 2022, arXiv e-prints, arXiv:2205.06269. <https://arxiv.org/abs/2205.06269>
- Finch, T. K., Carlivati, L. P., Winn, J. N., & Schechter, P. L. 2002, *ApJ*, 577, 51, doi: [10.1086/342163](https://doi.org/10.1086/342163)
- Kaplinghat, M., & Turner, M. S. 2001, *PhRvL*, 86, 385, doi: [10.1103/PhysRevLett.86.385](https://doi.org/10.1103/PhysRevLett.86.385)
- Keeton, C. R. 2001, arXiv e-prints, astro. <https://arxiv.org/abs/astro-ph/0102341>
- Luhtaru, R., Schechter, P. L., & de Soto, K. M. 2021, *ApJ*, 915, 4, doi: [10.3847/1538-4357/abfd1](https://doi.org/10.3847/1538-4357/abfd1)
- Malmquist, K. G. 1922, *Meddelanden fran Lunds Astronomiska Observatorium Serie I*, 100, 1
- Ohanian, H. C. 1983, *ApJ*, 271, 551, doi: [10.1086/161221](https://doi.org/10.1086/161221)
- Refsdal, S. 1964, *MNRAS*, 128, 307, doi: [10.1093/mnras/128.4.307](https://doi.org/10.1093/mnras/128.4.307)
- Rubin, V. C., Ford, W. K., J., Thonnard, N., Roberts, M. S., & Graham, J. A. 1976, *AJ*, 81, 687, doi: [10.1086/111942](https://doi.org/10.1086/111942)
- Schneider, P., & Sluse, D. 2013, *A&A*, 559, A37, doi: [10.1051/0004-6361/201321882](https://doi.org/10.1051/0004-6361/201321882)
- Shajib, A. J., Birrer, S., Treu, T., et al. 2019, *MNRAS*, 483, 5649, doi: [10.1093/mnras/sty3397](https://doi.org/10.1093/mnras/sty3397)
- Sharma, S. 2017, *ARA&A*, 55, 213, doi: [10.1146/annurev-astro-082214-122339](https://doi.org/10.1146/annurev-astro-082214-122339)
- Treu, T., & Marshall, P. J. 2016, *A&A Rv*, 24, 11, doi: [10.1007/s00159-016-0096-8](https://doi.org/10.1007/s00159-016-0096-8)
- Turner, E. L. 1980, *ApJL*, 242, L135, doi: [10.1086/183418](https://doi.org/10.1086/183418)
- Wong, K. C., Suyu, S. H., Chen, G. C. F., et al. 2020, *MNRAS*, 498, 1420, doi: [10.1093/mnras/stz3094](https://doi.org/10.1093/mnras/stz3094)